

Evolution of non-axisymmetric structures in protoplanetary discs

¹Enrico Ragusa, ¹Giuseppe Lodato, ^{1,2}Giovanni Dipierro, ³Giovanni Rosotti, ³Richard Booth, ³Cathie Clarke, ⁴Jean Teysandier, ⁵Daniel Price & ⁶Guillaume Laibe

¹Dipartimento di Fisica, Università Degli Studi di Milano, Via Celoria, 16, Milano, I-20133, Italy

²Department of Physics and Astronomy, University of Leicester, Leicester, LE1 7RH, UK

³Institute of Astronomy, University of Cambridge, Madingley Road, Cambridge, CB3 0HA, UK

⁴DAMTP, University of Cambridge, Cambridge CB3 0WA, UK

⁵Monash Centre for Astrophysics (MoCA) and School of Physics and Astronomy, Monash University, Clayton Vic 3800, Australia

⁶Univ Lyon, Univ Lyon1, Ens de Lyon, CNRS, UMR5574, F-69230, Saint-Genis-Laval, France

enrico.ragusa@unimi.it — Phone: +39 02 503 17226
giuseppe.lodato@unimi.it — Phone: +39 02 503 17449



UNIVERSITÀ DEGLI STUDI DI MILANO
DIPARTIMENTO DI FISICA

UNIVERSITY OF CAMBRIDGE
Department of Applied Mathematics and Theoretical Physics

Introduction

Recent spectacular observations of dust and gas in nearby protoplanetary discs with the Atacama Large Millimeter Array (ALMA) have revealed substructures in the form of crescent shaped features van der Marel et al. 2016, often explained in terms of vortices, that however require unphysically low levels of viscosity Ataiee et al. (2013). At the same time, recent extensive surveys of extra-solar planets around main sequence stars have revealed that planetary systems are often very eccentric, further indicating the importance of non axis-symmetric evolution of young protoplanetary systems. Indeed, the mutual exchange of energy and angular momentum between a planet and the disc can perturb the circular keplerian motion of the gas, leading naturally to the formation of non-axisymmetric features in the disc. Furthermore, these structures exert a backreaction on the companion that triggered their formation, causing a variation of the semimajor axis of the planet (migration) and of its eccentricity (see Kley & Nelson, 2012 for a review). In this poster I will present our results in this context.

Numerical Simulations

Two sets of numerical simulations, one using the 3D Smoothed Particle Hydrodynamics (SPH) PHANTOM (Price et al., 2017), the other using the grid code FARGO3D (Benítez-Llambay & Masset, 2016) in the 2D configuration. The SPH simulations (Ragusa et al., 2017) (black background panels in Fig. 1), consist in simulations of a gas+dust (one fluid model $St = t_s/t_{\text{dyn}} \ll 1$, where St is the Stokes number) disc ($q_d = M_d/M_* = 10^{-3}$) surrounding a binary object, using different binary mass ratios, in particular $q = \{0.01, 0.05, 0.1, 0.2\}$ and $\alpha_{SS} = 0.05$. The output is then processed the RADMC-3D Monte Carlo radiative transfer code (Dullemond, 2012) together with the Common Astronomy Software Application (CASA) ALMA simulator (version 4.5.3), focusing on ALMA band 7 (continuum emission at 345 GHz) (see Fig. 2) in order to obtain mock ALMA observations.

The grid simulations (white background panels in Fig. 1) consist instead of two very long time scales (one up to $t = 3 \times 10^5$ orbits) simulations of a binary with fixed mass ratio ($q = 0.013$, typical of a star + hot jupiter system), surrounded by a gaseous disc with $M_d/M_p = 1/5$ and $M_d/M_p = 3/5$, denoted as “light” and “massive” disc cases, respectively.

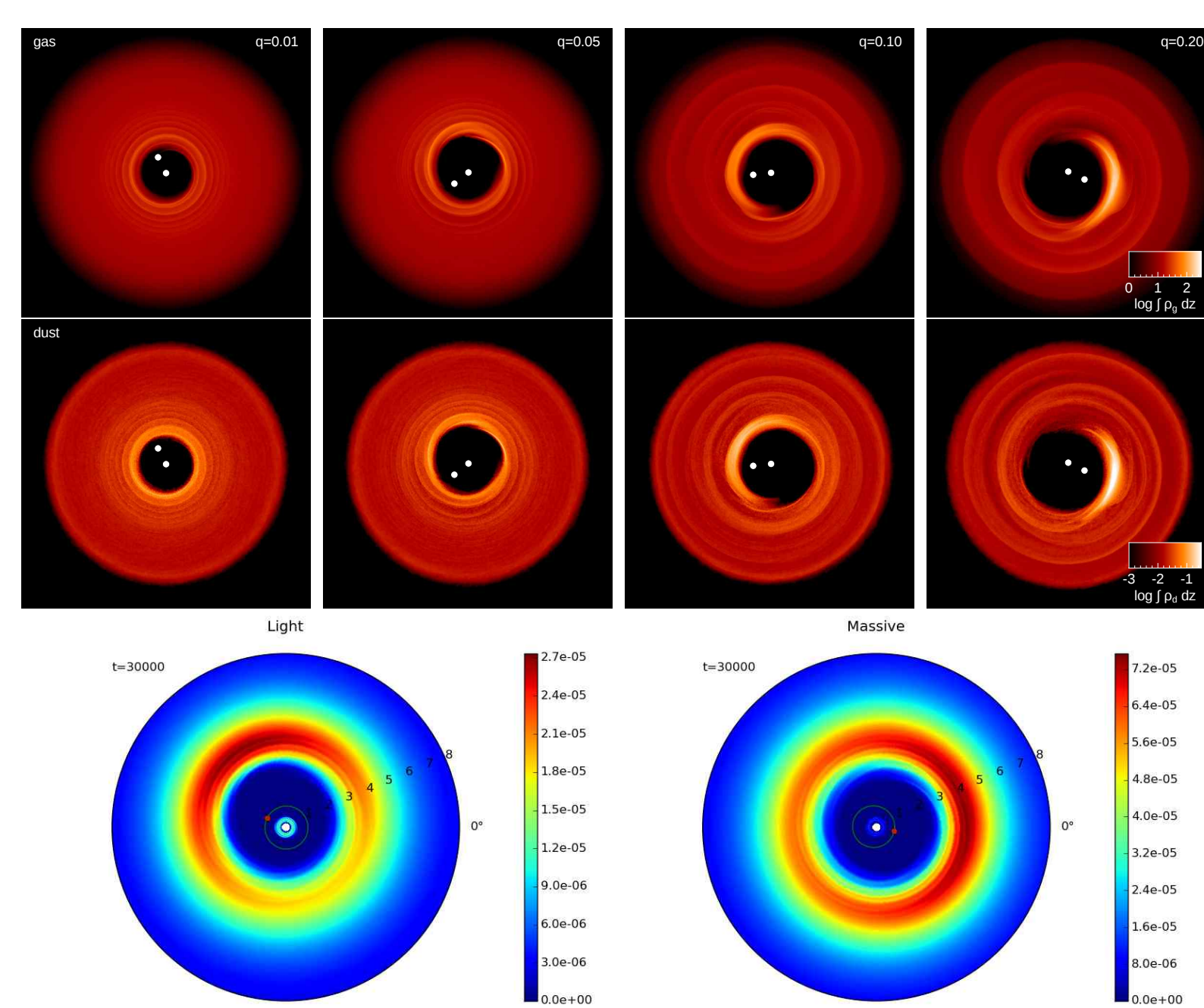


Figure 1: Top and middle rows: results of SPH simulations. Gas and dust surface density in units of g/cm^2 in logarithmic scale after 140 binary orbits for binary mass ratios $q = \{0.01, 0.05, 0.1, 0.2\}$ (left to right, respectively). High mass ratio binaries drive the formation of a large eccentric cavity leading to non-axisymmetric overdensities in both gas and dust ($q \gtrsim 0.05$). Low binary mass ratios produce more axisymmetric overdensities around a smaller central cavity. ($q \lesssim 0.05$; left columns). Bottom row: results FARGO3D simulations. Color plot of gas surface density in code units after 3×10^4 orbits. Left panel represents the light case ($M_d/M_p = 1/5$), the right one the massive one ($M_d/M_p = 3/5$). It can be noticed the formation of an eccentric, non-axisymmetric cavity carved by the planet.

Horseshoes in protostellar discs

The idea that large scale asymmetries might be due to a planetary companion was explored by Ataiee et al. (2013), who concluded that planetary mass objects only produce ring-like features in the disc, in contrast to the observed horseshoe. However, we have shown the dynamics induced in the disc by low and high mass companions is markedly different. It is known that low-mass companions, with $q \sim 10^{-3}$ can produce eccentric cavities, that precess slowly around the star-planet system (Kley & Dirksen, 2006). In contrast, more massive companions, with $q \gtrsim 0.04$ (Shi et al., 2012; D’Orazio et al., 2016; Ragusa et al., 2016) produce strong non-axisymmetric lumps that orbit at the local Keplerian frequency. For sufficiently massive companions (binary mass ratio $q = 0.2$) we obtain an azimuthal contrast of the order of ~ 10 in mm-wave map, with the contrast an increasing function of the binary mass ratio.

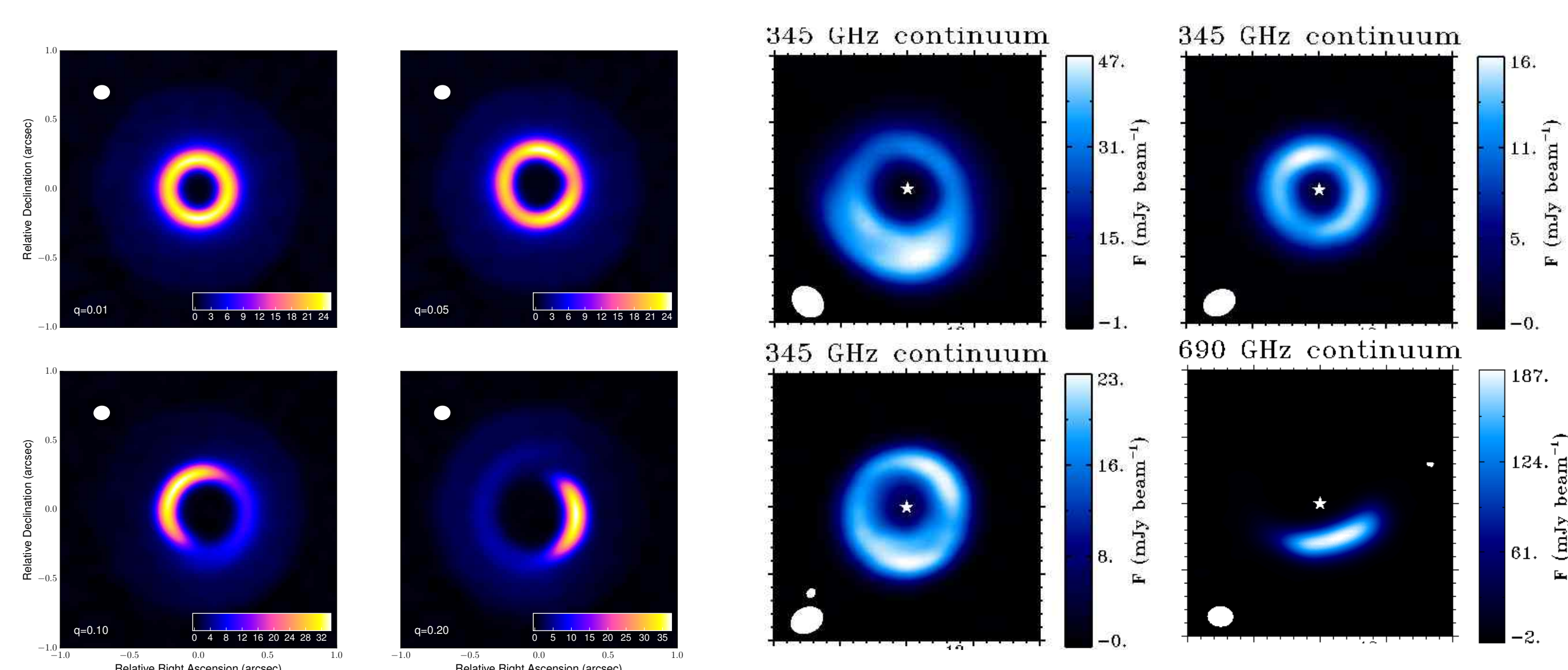


Figure 2: Comparison of ALMA simulated observations at 345 GHz of disc models (first and second columns from left) and real ALMA observations (third and fourth column from left) (van der Marel et al., 2016). Simulated images have mass ratios $q = 0.01$ (first top panel from left), $q = 0.05$ (second top panel), $q = 0.1$ (first bottom panel) and $q = 0.2$ (first bottom panel). Real images represent the objects HD135344B, DoAr44, SR21 and IRS48 (third and fourth columns top down). Intensities are in mJy beam^{-1} . The white colour in the filled ellipse in the upper left corner indicates the size of the half-power contour of the synthesized beam: 0.12×0.1 arcsec ($\sim 16 \times 13$ au at 130 pc.).

Name	Contrast	Dust trapping	Companion	Consistency
HD135344B	$\lesssim 10$	No	Strong indication	Yes
SR 21	$\lesssim 10$	No	Indication	Yes
DoAr 44	$\lesssim 10$?	?	Yes
IRS 48	$\gtrsim 100$	Yes	?	No
HD142527	~ 30	cm grains?	Yes	Yes
Lk H α 330	$\lesssim 10$?	Indication	Yes

Table 1: Summary of transition discs displaying horseshoe or other non-axisymmetric features. For each source, we indicate the observed contrast in mm images, whether there is evidence for dust trapping in the crescent, and whether the system is known to host a massive companion. The last column indicates whether the observed structures are consistent with our model, given the upper-limits on the companion mass as reported in the literature.

Planetary eccentricity growth during disc migration

In the following equations we will use the following notation $E_j = |E_j|e^{i\Phi_j}$, $j = \{p, d\}$, where $|E_j| = e_j$ is the “physical” eccentricity and Φ_j is its pericentre phase, the pedices p and d refer to the planet and disc-“virtual” planet. In fact, we generalize the equations ruling the planet disc interaction Teysandier & Ogilvie (2016) treating the disc as if it was a second planet undergoing secular interaction with the first one. The equations ruling the evolution of the complex eccentricities E_p and E_d have the form (Zhang et al., 2013)

$$\begin{pmatrix} \dot{E}_p \\ \dot{E}_d \end{pmatrix} = i\Omega_{\text{sec}} \begin{pmatrix} q & -q\beta \\ -\sqrt{\alpha}\beta & \sqrt{\alpha} \end{pmatrix} + \mathcal{G} \begin{pmatrix} \lambda_{11} & \lambda_{12} \\ \lambda_{21} & \lambda_{22} \end{pmatrix} \cdot \begin{pmatrix} E_p \\ E_d \end{pmatrix}, \quad (1)$$

where the notation \dot{E}_j indicates the eccentricity time derivative, $\alpha = a_p/a_d$, $q = M_d/M_p$, $\beta = b_{3/2}^{(2)}(\alpha)/b_{3/2}^{(1)}(\alpha)$ and $b_{3/2}^{(n)}(\alpha)$ is the n -th Laplace coefficient. The solutions to equation (1) are in the form

$$\begin{pmatrix} E_p(t) \\ E_d(t) \end{pmatrix} = C_1 \begin{pmatrix} \eta_+ \\ 1 \end{pmatrix} e^{ig_+t} + C_2 \begin{pmatrix} \eta_- \\ 1 \end{pmatrix} e^{ig_-t}, \quad (2)$$

where C_1 and C_2 are constants that depend on the initial conditions, $g_{\pm} = \varpi_{\pm} + i\gamma_{\pm}$ and $(\eta_{\pm}, 1)$ are the complex eigen-values and complex eigen-vectors of the sum of the matrices in eq. (1).

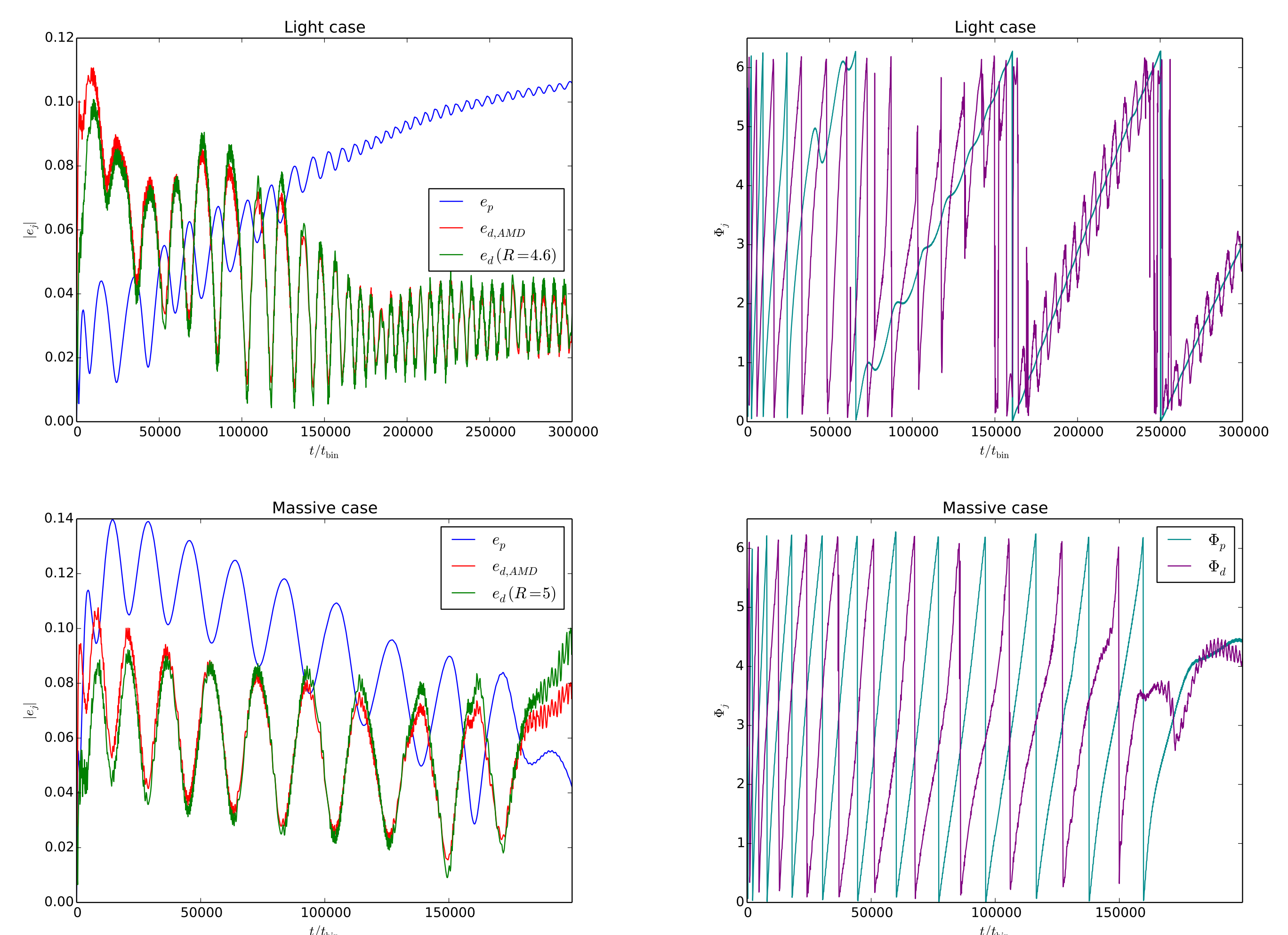


Figure 3: Eccentricity e as a function of time for light (top panel) and massive (bottom panel) case. The blue curve shows the planet eccentricity, the green curve the disc eccentricity at $R = 4.5$ in the light case and at $R = 5$ in the massive one, finally the red curve estimates the global amount of the disc eccentricity during the first stages of evolution ($t \lesssim 1.5 \times 10^4$ orbits) of the system up to values $e_d \sim 0.11$, then a slower decrease at later times. The planet eccentricity in the massive case shares a similar behavior: it grows fast in the beginning, hits a value $E_p = 0.14$ and start decreasing at the same rate as the disc eccentricity. The planet eccentricity in the light case in contrast has a completely different behavior: the growth of the planet eccentricity oscillates around $E_p = 0.025$ for $t < 5 \times 10^4$ orbits, but then at later times starts growing again at constant rate.

Figure 4: pericentre phase as a function of time for light (top panel) and massive (bottom panel) case. The cyan and violet curve represent planet and disc pericentre phase. It can be shown that the disc pericentre phase do not depend on the radius, in fact showing a rigid precession. During the first 4×10^4 orbits both simulations show an anti-aligned precession ($|\Phi_p - \Phi_d| \approx 180^\circ$). After 4×10^4 orbits in the light case the planet precession decouples from that of the disc: the planet precession rate becomes much slower than that of the disc. At very late times ($t > 2 \times 10^5$ orbits) in the light case also the disc precession rate slows down, and the gas orbits precess along the planet one in a pericenter aligned configuration. The massive case remain in the anti-aligned configuration much longer even though also in this case a transition toward the slow aligned configuration is likely taking place at $t \sim 2 \times 10^5$.)

Conclusions

- We propose a new model to account for the horseshoes features often observed in transitional discs. In this model, the structures are a direct probe of the presence of an unseen binary companion at small radii (see Tab. 1).
- Non-axisymmetric features can be formed also by sufficiently massive ($q > 0.1$) binary companions in the mass regime of brown dwarfs without requiring the vortex scenario and low disc viscosities (Ragusa et al., 2017).
- We demonstrate that planet-disc interaction during planetary migration can induce a significant planetary eccentricity, potentially explaining some of the high eccentricities discovered in recent years in the exoplanetary population.
- The system undergoes secular eccentricity oscillations visible on long timescales ($t > 1.5 \times 10^4$ orbits), and the global eccentricity growth/decrease trend depends apparently also on secular planet-disc interaction.

References

- Ataiee S., et al., 2013, A&A, 553, L3
Benítez-Llambay P., Masset F. S., 2016, ApJS, 223, 11
D’Orazio D. J., et al., 2016, MNRAS, 459, 2379
Dullemond C. P., 2012, Astrophysics Source Code Library (ascl:1202.015)
Kley W., Dirksen G., 2006, A&A, 447, 369
Kley W., Nelson R. P., 2012, ARA&A, 50, 211
Price D. J., et al., 2017, preprint, (arXiv:1702.03930)
Ragusa E., Lodato G., Price D. J., 2016, MNRAS, 460, 1243
Ragusa E., Dipierro G., Lodato G., Laibe G., Price D. J., 2017, MNRAS, 464, 1449
Shi J.-M., Krolik J. H., Lubow S. H., Hawley J. F., 2012, ApJ, 749, 118
Teyssandier J., Ogilvie G. I., 2016, MNRAS, 458, 3221
Zhang K., Hamilton D. P., Matsumura S., 2013, ApJ, 778, 6
van der Marel N., et al., 2016, A&A, 585, A58